

# Strain rate-sensitive analysis for grinding damage of brittle materials

Chongjun Wu<sup>1,2</sup> · Beizhi Li<sup>1</sup> · Yao Liu<sup>1</sup> · Jingzhu Pang<sup>1</sup> · Steven Y. Liang<sup>2</sup>

Received: 4 May 2016 / Accepted: 25 July 2016 / Published online: 10 August 2016  
© Springer-Verlag London 2016

**Abstract** Grinding of brittle materials will inevitably cause grinding damages characterized by fracture microcracks, which will greatly affect the grinding integrity. Traditional damage models are just concerned about the material properties and interaction depth between grit and workpiece without considering the dynamic effect on material strength. This paper proposed new damage analysis models which consider the effect of both strain rate and grinding parameters on grinding damages. It is believed that the material strength and dynamic fracture toughness vary under different grinding parameters due to the variation of strain rate brought by the grinding speed and chip thickness. By introducing the grinding-induced strain rate, the new damage models were further updated as the function of the grinding speed and chip thickness. The grinding damage models were verified through different grinding tests. Combining with the surface roughness results, the grinding damages under different grinding speed and damages are fully discussed. Finally, the damage-free grinding was proposed based on the proposed model. It can be concluded that a combination of the grinding speed and reduction of the chip thickness can help achieve damage-free ground surface.

**Keywords** Grinding damage · High-speed grinding · Silicon carbide · Strain rate · Surface roughness

✉ Jingzhu Pang  
pangjz@dhu.edu.cn

<sup>1</sup> School of Mechanical Engineering, Donghua University, 201620 Shanghai, China

<sup>2</sup> Manufacturing Research Center, Georgia Institute of Technology, 30332 Atlanta, USA

## 1 Introduction

Silicon carbide ceramics are now being widely used in engineering applications such as bearings, valves, and electronics for their high hardness, excellent wear resistance, and extremely high-temperature strength [1]. Diamond grinding [2, 3] is generally considered as the main machining method to obtain a desired dimensional tolerance and surface integrity in precision engineering. However, due to the hard and brittle nature of the brittle materials, machining of this ultra-hard ceramic material will inevitably cause microcracks and surface/subsurface damages [4] which will deteriorate surface quality [5] and further affect the effective use of these materials in structural applications [6]. Therefore, in order to inhibit grinding damages, a good understanding of damage mechanism under different process parameters is necessary.

In the study of brittle material grinding, the indentation fracture mechanics approach likens abrasive-workpiece interactions for grinding of ceramics to small-scale indentation events [7]. In indentation of brittle materials, there exist generally two principal crack systems [8], the lateral and median cracks. They are formed after the plastic deformation between the grit and the workpiece. Lawn et al. [9] developed a theory for describing the evolution of the median/radial crack system in the far field of sharp indenter contacts considering the complex elastic/plastic field beneath the indenter. Lambropoulos et al. [10] presented the theoretical calculation function of lateral and median cracks based on micro-indentation mechanics. Based on Lambropoulos' model, Li et al. [11] and Yao et al. [12] modeled the relationship between subsurface damage and surface roughness of optical materials in grinding processes. Gu et al. [13] established a model for the correlation between the depth of the subsurface cracks and the scratch depth through scratch tests of optical glass BK7. Subsequently, Lin et al. [14] investigated the surface integrity during diamond grinding of BK7. However, the above works

for investigations of grinding damages are mainly conducted under a conventional grinding speed with a static description of induced grinding damages.

The grinding wheel speed was used as a parameter to inhibit surface crack generation [15] in the grinding of brittle materials. Wang et al. [16] developed a new model for the relationship between the grinding damage and grinding parameters in high-speed grinding of brittle materials. But, there is no theoretical explanation or consideration of the strain rate effect brought by the grinding wheel speed and chip thickness. This does not match the real situation of the grinding process. In the high-speed grinding of brittle materials, the increase of the wheel velocity will definitely enhance the strain rate of the material when the grinding wheel interacts with the workpiece. It has been reported that the increase of the strain rate will greatly affect the material mechanical properties, especially for strength [17]. The fracture stress will increase with increasing strain rate in monolithic and composite ceramic materials [17, 18]. Therefore, in order to fully evaluate the damages in grinding processes, the strain rate effect brought by the increased wheel speed should be fully discussed.

From the above literature review, it is obvious that the strain rate has a great effect on the material properties and should be considered in the study of grinding damages. Therefore, this paper is devoted to evaluate the damage mechanism by considering both the grinding parameters and strain rate effect brought by the wheel speed and chip thickness. The indentation fracture mechanics theory was applied to explain the grinding mechanism and obtain general damage models considering the chip thickness. Furthermore, the strain rate was incorporated into the damage model in the function of a combination of grinding speed and chip thickness. Finally, high speed grinding experiments were conducted to verify the proposed damage model through SEM observations of both the surface and subsurface damages. Moreover, 3-D topology surface roughness data were also given to explain the speed and chip thickness effect in grinding processes. A final discussion of damage-free grinding of brittle materials helps to provide more in-depth understanding of grinding mechanism for brittle materials.

### 1.1 General description of damage formation in grinding processes

In grinding of brittle materials, the interaction between the abrasive grit and workpiece can be regarded as a scratch process [12–14]. The geometrical damage formation schematic can be seen in the Fig. 1. As shown in Fig. 1, two different crack systems will be produced when the grit scratches across the workpiece, the lateral crack and median crack. It is generally believed that brittle materials are removed by the formation of lateral crack beneath the contact compression, at a depth in the plastic zone, followed by the subsequent outward

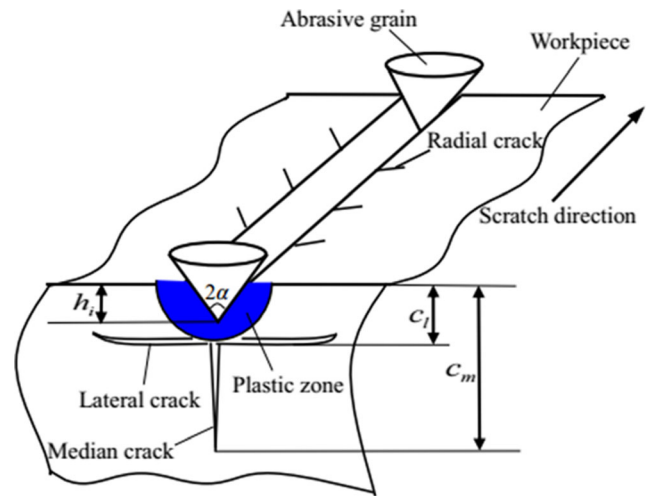


Fig. 1 Grinding damages in the scratch process [12, 16]

propagation of lateral crack and final emergence to the material surface [16]. The theoretical equation of lateral crack depth  $C_1$  can be expressed as a function which is related to the material properties and the interaction depth between the wheel and workpiece [19].

$$SD = C_1 = \left[ \frac{3(1-2\nu)}{5-4\nu} + \frac{2\sqrt{3}}{\pi(5-4\nu)} \frac{E}{\sigma_c} \cot\alpha \right]^{1/2} \tan\alpha \cdot h_i \quad (1)$$

where  $E$  is the elastic modulus,  $h_i$  represents the interaction depth between the abrasive grit and the material. In grinding processes, it represents the chip thickness.  $\nu$  and  $\sigma_c$ , respectively, are the Poisson's ratio and the yield strength in compression test.  $\alpha$  is the semi-included angle of the abrasive grain (as illustrated in Fig. 1), it is given  $60^\circ$  [20]. In the grinding process, the lateral crack is generally reflected by the surface crack size, which will greatly affect grinding surface roughness.

The median crack extends perpendicularly to the grinding surface with a sharp indenter, and it is considered as the main type of the subsurface crack [16]. The median crack length is similar to the lateral crack length. The theoretical equation of median crack depth  $C_m$  can be given as follows [13].

$$SSD = C_m = 0.206 \frac{(E \cdot H)^{1/3}}{(K_{IC} \cdot \beta)^{2/3}} (\cot\alpha)^{4/9} (\tan\alpha)^{4/3} \cdot h_i^{4/3} \quad (2)$$

where  $H$  is the scratch hardness,  $K_{IC}$  is the fracture toughness and  $\beta$  is a material parameter determined by elastic recovery.

In the grinding process, the interaction depth  $h_i$  will not be higher than the maximum undeformed chip thickness  $h_m$  and the maximum theoretical damage crack size would be the interaction depth  $h_i$  is equal to the chip thickness  $h_m$ . The chip

thickness was used to characterize the depth of penetration for a single grit and can be given as follows [21].

$$h_m = \left( \frac{3}{C_d \cdot \tan \alpha} \cdot \frac{V_w}{V_s} \cdot \sqrt{\frac{a_e}{d_e}} \right)^{\frac{1}{2}} \tag{3}$$

where  $C_d$  represents the active abrasive grits number in unit area.  $V_s$  and  $V_w$ , respectively, represents the wheel speed and workpiece peripheral speed  $a_e$  is the depth of cut,  $d_e$  is the equivalent diameter,  $d_e = d_s \cdot d_w / (d_s + d_w)$ .  $d_w$  represents the workpiece diameter and  $d_s$  is the wheel diameter. The value of  $C_d$ , in Eq. (2), can be derived as follows [3]:

$$N_d = 4\chi / \left\{ d_g^2 (4\pi/3\omega)^{2/3} \right\} \tag{4}$$

where  $d_g$  is the equivalent spherical diameter of diamond grit,  $\omega$  is the volume fraction of diamond in the grinding wheel and volume fraction  $\omega$  is 0.375 when the grinding wheel in this paper has a density of 150 [22].  $\chi$  is the fraction of diamond particles that actively cutting in grinding. The active grits are assumed that one third of the total abrasive particles are actively engaged in cutting [23], or the value of  $\chi$  is given 1/3.

### 2 Strain rate effect in damage evaluation

In the previous damage model (1) and (2), it can be found that the grinding damage was only dependent on the indentation depth and material properties. However, the machining process is a dynamic process; the variation of strain rate brought by the wheel speed has been proved to have a corresponding effect on the material strength [17, 24, 25]. Therefore, the strain rate effect should be fully considered. It is suggested that the compression failure strength in the high strain rate regime is highly strain rate sensitive and it is given as follows [17, 26]:

$$\sigma_c = \sigma_0 + B \left( \dot{\varepsilon} \right)^{1/3} \tag{5}$$

where  $\dot{\varepsilon}$  is the strain rate exerted on the material,  $\sigma_0$  is the static compression strength and  $B$  is a constant. The strain rate is used to characterize the deformation velocity of the workpiece material; it is the derivative of the strain to the time. In the high-speed grinding, the increase of the grinding speed will lead to an increase of the strain rate substantially and the strain rate can be calculated through the wheel speed divided by specimen length  $l_s$ . It can be expressed as follows [27, 28]:

$$\dot{\varepsilon} = \frac{V_s}{l_s} \tag{6}$$

In the grinding process, the specimen length  $l_s$  is highly related to the grinding wheel type, topology, process parameters and workpiece material. It can be expressed as [17]:

$$l_s = k_1 \cdot h_m \tag{7}$$

where  $k_1$  is a constant which is decided by the wheel type, topology, and workpiece material. According to Eqs. (5), (6), and (7), the new description of the strain rate-sensitive compressive strength can be given as follows.

$$\sigma_c = \sigma_0 + B \left( \frac{V_s}{k_1 \cdot h_m} \right)^{1/3} \tag{8}$$

For further investigation of the fracture toughness of the brittle materials from dynamic fracture toughness model proposed by Liu et al. [24], the fracture toughness has the following correlation with the strength.

$$\sigma_c = \frac{K_{IC}}{\sqrt{\pi L (1-\nu^2)}} \tag{9}$$

where  $L$  is crack length in static condition, it is a material constant. Therefore, combining Eqs. (8) and (9) and with Eqs. (1) and (2), the damage evaluation model considering the effect of strain rate and grinding parameters can be obtained. For expression simplification, the constant will all be brought out and substituted by a new constant.

$$\begin{cases} C_1 = \left[ \frac{3(1-2\nu)}{5-4\nu} + \frac{2\sqrt{3}}{\pi(5-4\nu)} \frac{E}{\sigma_0 + \lambda(V_s/h_m)^{1/3}} \cot \alpha \right]^{1/2} \tan \alpha \cdot h_m \\ C_m = \frac{(E \cdot H)^{1/3}}{k \left( \sigma_0 + \lambda(V_s/h_m)^{1/3} \right)^{2/3}} (\cot \alpha)^{4/9} (\tan \alpha)^{4/3} \cdot h_m^{4/3} \end{cases} \tag{10}$$

In the above damage model,  $k$  and  $\lambda$  are the material constants and they will be obtained through experiments. From this model, it can be found that both the grinding speed and chip thickness are the main factors that will affect the grinding damages. When the chip thickness is kept constant, the increase of the grinding wheel speed will diminish the grinding damage depth, while when the grinding speed is kept constant, the enhancement of the chip thickness will increase the material removal rate, and thus, the grinding damage will get higher.

### 3 Experiments

The experimental conditions are given in Table 1. The grinding machine spindle is capable of running up to 8000 rpm with a 400-mm wheel. The spindle drive motor power can reach up to 41.9 kw. The reaction-sintered SiC in Table 2 was used for investigation. And, the workpiece specimens have a diameter of  $\Phi 60$  mm with a width of 20 mm. The grinding wheel was

**Table 1** Grinding conditions

Type	Content
Machine tool	CNC cylindrical grinding machine MGKS1332/H
Grinding wheel	Vitrified Diamond Wheel D91 V+ 2046 JISC-23 C150 E
Wheel width	22 mm
Machining mode	Plunge Up grinding
Wheel speed	20–150 m/s
Workpiece speed	300–1200 mm/min
Depth of cut	2–20 $\mu\text{m}$
Cooling	Water-based emulsion 5 % at the speed of 10 L/min
Wheel spindle balancing system	Model SB-4500 under 0.03 $\mu\text{m}$

balanced below 0.03  $\mu\text{m}$  at the grinding speed with a dynamic balancing instrument (Model-SB-4500) installed on the spindle. The grinding wheel was trued using a diamond truer and dressed using an alumina stick of 200-mesh size for 30s under a coolant before every set of test was undertaken. The grinding surface and subsurface damages were observed through an environment scanning electron microscope (ESEM) QUANTA 250 from Czech. Before observation, the workpiece was first polished and then cleaned with acetone in an ultrasonic bath for at least 20 min. Moreover, the surface roughness was measured through a Bruker Nano Surface white light interferometer (Npflex). In Fig. 2, the detailed experiments were established on a cylindrical grinding machine. In this figure, the specimen was given in Fig. 2(a). The quarter part was used to observe the surface and subsurface damages. The contact area between the two parts was the polished area for subsurface damage observation on a scanning electron microscope.

## 4 Results and discussions

### 4.1 Grinding damages under different grinding speed and chip thickness

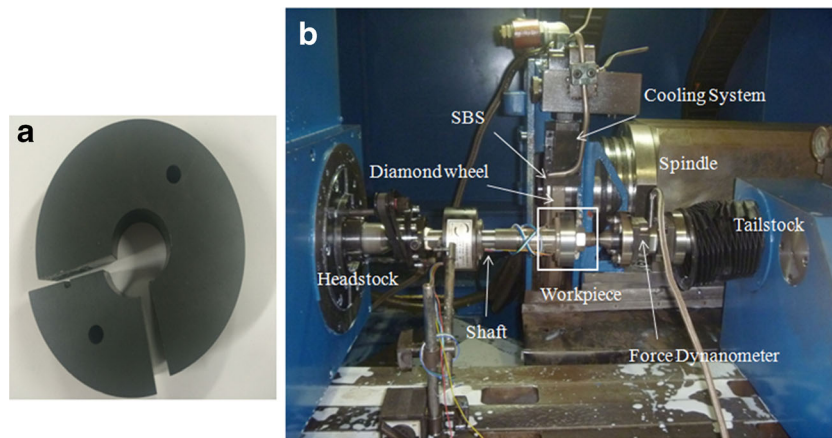
From formulas (1) and (2) in chapter 2, the grinding damages were only dependent on the material properties and chip thickness between the grit and workpiece, which means that if the chip thickness is kept constant, the grinding damages will not change when the wheel speed varies. From the SEM results in

Fig. 3, this does not fit the real observation results. Therefore, the surface and subsurface damages considering both the chip thickness and grinding speed were given in the SEM topology pictures in Fig. 3. It can be found from Fig. 3a, b that when the wheel speed increases, the surface damage crack size will get inhibited and the damage area will get smaller; more plastic striations can be found in Fig. 3b compared with fracture cracks in Fig. 3a. This is because the increase of the grinding speed will promote the strain rate in the grinding process, which will further enhance the material strength. Thus, a reduction of the surface damage is quite easy to understand from damage model in formula (9). However, the chip thickness shows a different influence on the surface damage in Fig. 3c. Comparing with Fig. 3b at a chip thickness of 0.52  $\mu\text{m}$ , the surface fracture cracks in Fig. 3c get much bigger. This can be understandable from formula (9) that the increase of the chip thickness will increase the interaction depth between the grit and workpiece, which will cause a higher grinding force and, thus, more severe damages.

For the subsurface damages, the grinding speed and chip thickness shows the same physics with the surface damage. In Fig. 3d–f, the direction for (e) is different with (d) and (f) because the placed position of specimen is different. Two small parts in Fig. 1a were placed against together to keep flat when doing the SEM tests. In Fig. 3, in order to clearly measure the crack size of surface/subsurface damage, different magnifications for SEM figures were applied. The wheel speed effect in Fig. 3d, e shows that the increase of grinding speed can be used to inhabit the subsurface damage. While the chip thickness has a negative effect on the subsurface damages

**Table 2** Mechanical properties for SiC

Material properties for SiC					
	Density	Compressive strength	Hardness	Fracture toughness	Elastic modulus
	$\rho$ [g/cm <sup>3</sup> ]	$\sigma_c$ [MPa]	$H$ [GPa]	$K_{1C}$ [MPa.m <sup>1/2</sup> ]	$E$ [GPa]
SiC	3.22	2600	23	410	0.16



**Fig. 2** SiC workpiece (a) and experiments setup (b)

in Fig. 3e and f. That is to say, in order to improve the surface quality and reduce grinding damages, the increase of grinding speed combined with the decrease of the chip thickness can be adopted. In order to calibrate and verify the reasonability of the strain rate sensitive damage model in formula (9), a group of experimental results are given in Table 3. In this table, the SD and SSD values are average data of three different tests. Based on the first five groups of experimental data in Table 3, the constants  $k$  and  $\lambda$  in formula (9) can be calculated. It is 0.07 for  $k$  and 0.3 for  $\lambda$ . In this table, the error of experimental value over the predicted value are given to show the prediction accuracy. The results show that the predicted values from formula (9) match very well with the experimental results.

This proves that both the strain rate effect and interaction depth should be considered in the damage analysis.

### 4.2 Grinding surface roughness

Surface roughness is one of the most important factors in assessing the quality of a machined surface. In the grinding of brittle materials, it is inevitable to cause grinding damages. These damages are the main factors that affect the surface roughness. Therefore, the surface roughness can be used as a parameter to characterize and indicate the grinding damage. In this paper, a 3-D Bruker Nano Surface white light interferometer (Npflex)

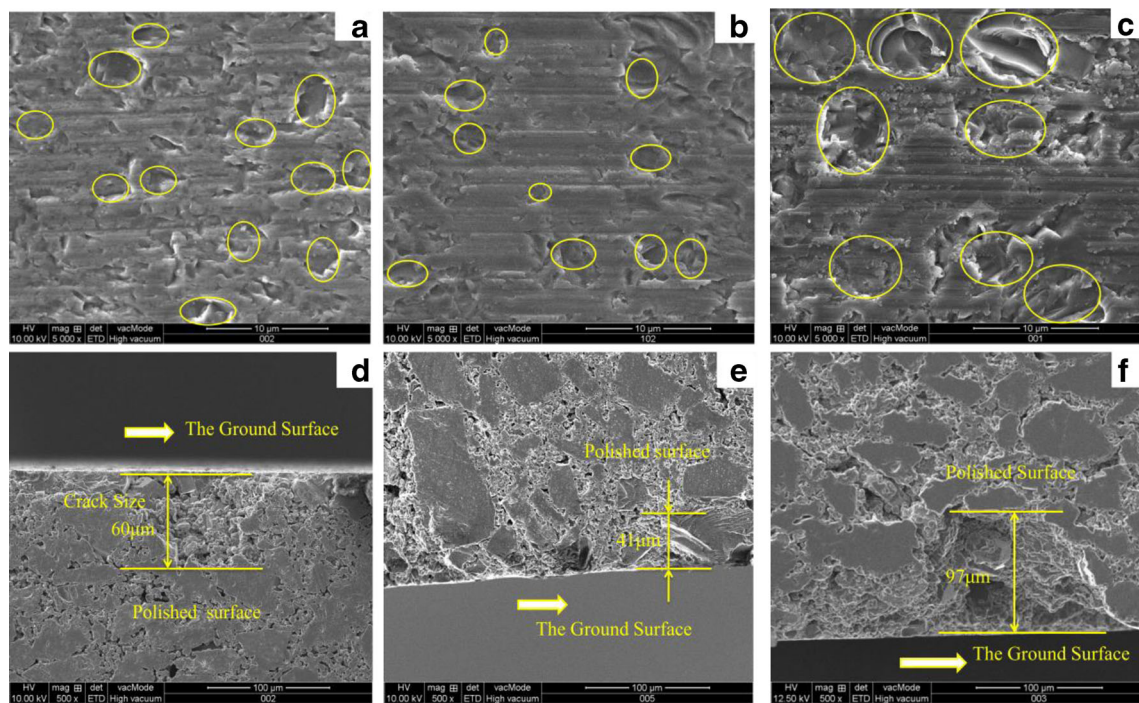


**Fig. 3** Surface/subsurface damage SEM topology for SiC at a and d  $V_s = 80$  m/s,  $h_m = 0.52 \mu\text{m}$ ; b and e  $V_s = 140$  m/s,  $h_m = 0.52 \mu\text{m}$ ; c and f  $V_s = 140$  m/s,  $h_m = 1.04 \mu\text{m}$ ; a–c  $\times 5000$ ; and d–f  $\times 500$

**Table 3** Experimental results and its error with predicted value

Experimental No.	Wheel speed $V_s$ (m/s)	Chip thickness $h_m$ ( $\mu\text{m}$ )	Experimental SD ( $\mu\text{m}$ )	Error with predicted value (%)	Experimental SSD ( $\mu\text{m}$ )	Error with predicted value (%)
1	80	0.52	3.7	6	58	13
2	140	0.52	3.5	3	39	2
3	140	1.04	7.2	3	94	12
4	80	0.68	5.2	5	70	3
5	80	0.81	5.9	6	103	4
6	140	0.16	1.1	12	7	11
7	140	0.31	1.7	5	23	8
8	20	0.89	6.8	3	114	7

was used to measure the surface roughness value. The 3-D topology of the surface roughness and the values are given in Fig. 4. In this group of figures, the effect of grinding speed and chip thickness will be discussed. It can be seen from the Fig. 4a, b that when the grinding speed increases from 80 to 140 m/s, the surface roughness drops from 0.297 to 0.187  $\mu\text{m}$ . Moreover, the surface topology at a higher grinding speed (140 m/s) has better surface finish and less pits and grooves than the picture in the lower speed (80 m/s). Figure 4b–d can explain the chip thickness effect on the surface roughness. The surface roughness at chip thickness of 1.04  $\mu\text{m}$  is 0.317  $\mu\text{m}$  (Fig. 4c), while it is 0.187  $\mu\text{m}$  at a chip thickness of 0.52  $\mu\text{m}$  (Fig. 4b) and 0.165  $\mu\text{m}$  at chip thickness of 0.32  $\mu\text{m}$  (Fig. 4d). The above results from the surface roughness show the same mechanism from the grinding damage. Therefore, it can be concluded that the increase of the grinding speed helps to

inhibit the grinding damages and improve the surface quality. However, the reduction of the chip thickness helps increase the surface quality. Thus, in order to achieve higher surface quality, it can be suggested that a combination of the increase of the grinding speed and control of the chip thickness can be adopted.

#### 4.3 Discussions of the damage-free grinding for SiC

In order to achieve damage-free and high-quality products without post processing, ductile-regime machining was put forward for brittle materials. This kind of machining mode can generate the chips through a mode of plastic deformation rather than fracture, and thus, a higher accuracy of the machined surface can be obtained. Bifano et al.[27] have proposed that ductile grinding

**Fig. 4** Ground surface morphology of SiC. **a**  $V_s = 80$  m/s,  $h_m = 0.52$   $\mu\text{m}$ . **b** 140 m/s,  $h_m = 0.52$   $\mu\text{m}$ . **c**  $V_s = 140$  m/s,  $h_m = 1.04$   $\mu\text{m}$ . **d**  $V_s = 140$  m/s,  $h_m = 0.32$   $\mu\text{m}$ . The arrows indicate the grinding direction

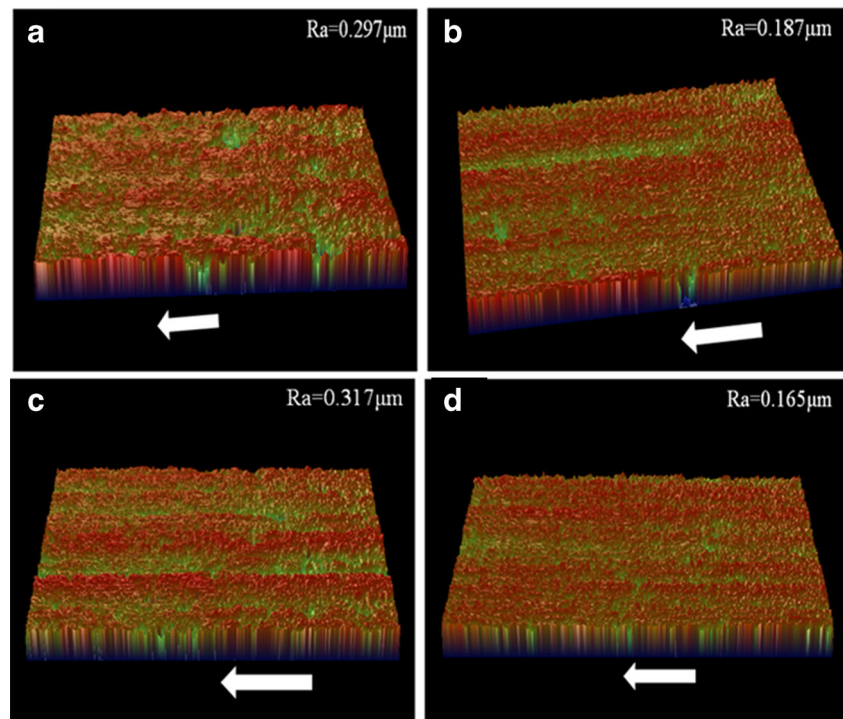
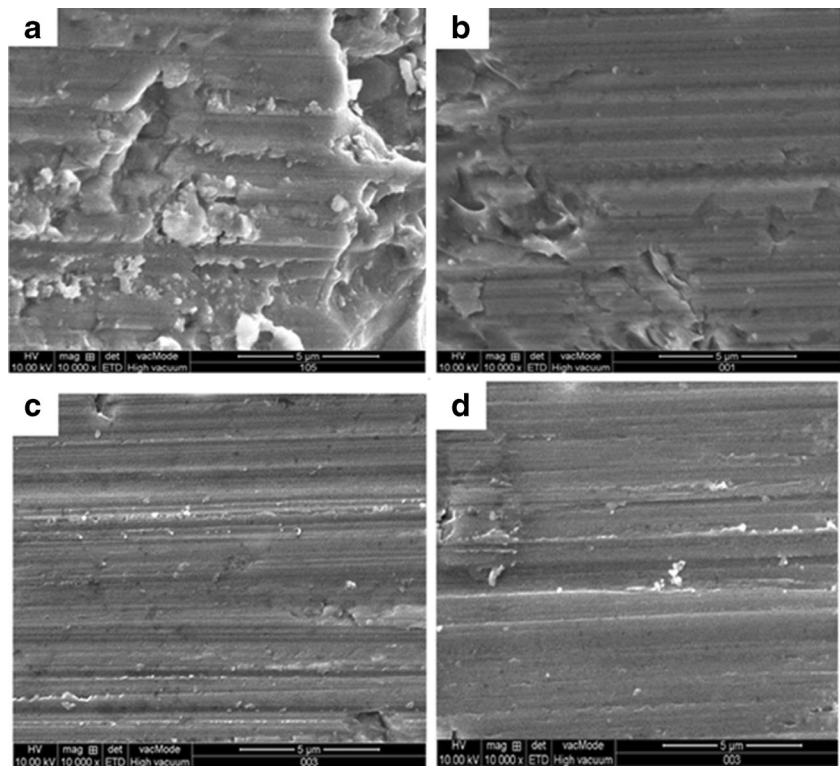


**Fig. 5** Damage-free grinding of SiC under a higher grinding speed (140 m/s). **a**  $h_m = 1.8 \mu\text{m}$ , 60 % fracture. **b**  $h_m = 1.04 \mu\text{m}$ , 32 % fracture. **c**  $h_m = 0.32 \mu\text{m}$ , 8 % fracture. **d**  $h_m = 0.16 \mu\text{m}$ , 4 % fracture



could be achieved in the machining of brittle materials when the chip thickness is small enough. And the critical depth for ductile grinding  $d_c$  was given [27]:

$$d_c = \beta \left( \frac{E}{H} \right) \cdot \left( \frac{K_{IC}}{H} \right)^2 \tag{11}$$

where  $\beta$  is a constant ( $\beta = 0.15$  [27]),  $E$  is the elastic modulus, and  $H$  is the hardness. The experiments in this model were conducted under a constant grinding speed of 26.2 m/s. It can be found that this model is fully dependent on the material properties. Moreover, the critical value for ductile grinding of SiC is  $0.045 \mu\text{m}$ , which means that only when the chip thickness  $h_m$  is not higher than  $0.045 \mu\text{m}$ , the ductile grinding of SiC can be realized. According to this model, the ductile grinding can only be obtained at a very low chip thickness and very small material removal rate. It is very inefficient. However, in the previous chapters of this paper, it has been verified that different grinding parameters will cause the variation of the material strength and the fracture toughness. Thus, the grinding parameters should be considered in this model.

In chapter 5.1, it has been proved that the increase of the grinding speed will reduce the grinding damages. Thus, in order to obtain the damage-free surface, a higher grinding speed under low chip thickness should be adopted. Figure 5 gives the SEM observation results under different chip thickness. In this figure, a grid-

counting technique [3, 27] was adopted to calculate the fracture surface percentage. In this method, the whole SEM picture was divided into hundreds of squares. Then, the fracture surface proportion can be obtained through a selection of the fractured squares. It can be easily seen that the ground surface shows less grinding debris and fracture region with the decrease of  $h_m$ , from 1.8 to  $0.16 \mu\text{m}$ . When the  $h_m$  is  $1.8 \mu\text{m}$ , the fracture surface consists of 60 % of the whole ground surface, then a slightly decrease to 32 % for  $1.04 \mu\text{m}$ . However, when  $h_m$  decrease from  $1.04 \mu\text{m}$  to  $0.32 \mu\text{m}$ ,

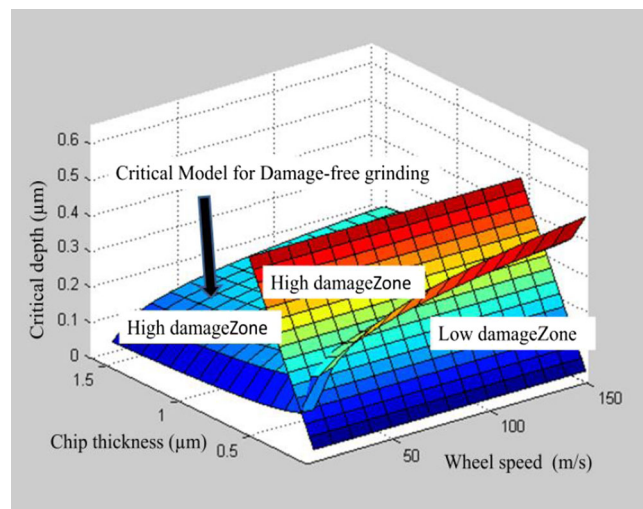


**Fig. 6** 3-D model for damage-free grinding considering the effect of grinding speed and chip thickness

the ground debris and fracture surface shows a substantially reduction, from 32 to 8 %. After that, when  $h_m$  continues to decrease, the ground surface shows a less grinding fracture. This can clearly conclude that the damage-free grinding of brittle materials can be realized at a combination of higher grinding speed and low grinding chip thickness. And, this chip thickness is much higher than the critical depth of  $0.045 \mu\text{m}$  in equation (11). Thus, the material removal rate can be greatly improved.

The new model was established by substituting the fracture toughness  $K_{1C}$  in equation (9) and compressive strength  $\sigma_c$  in equation (8) into the model (11). Then the new critical model for silicon carbide can be given as follows:

$$d_{nc} = \beta' \left( \frac{E}{H} \right) \left( \frac{\sigma_0 + 0.3(V_s/h_m)^{1/3}}{H} \right)^2 \quad (12)$$

where  $d_{nc}$  represents the new chip thickness model considering the strain rate sensitivity.  $\beta'$  is the material constant. According to the calibration of model (10), the constant  $\beta'$  can be given 0.4 for SiC.

Based on the new critical chip thickness model (12), the three dimensions (3-D) description for the new critical depth model considering the grinding speed and chip thickness was plotted in Fig. 6. In Fig. 6, the curved surface is the critical value for the predictive damage-free model, while the plane is the criterion that the chip thickness  $h_m$  is equal or below to the critical value. It is obvious that the increase of the wheel speed will lead to an increase of the critical value, while the chip thickness shows a negative trend. Moreover, the damage-free zone is under the new critical model curved surface when the chip thickness  $h_m$  is equal or smaller than the critical value, and it is indicated in the outward part of the space intersection between the two surfaces. The remains are the zones that may cause high surface damages.

## 5 Conclusions

Grinding damages in brittle materials are always the main factors that affect the machining quality. This is because that it is inevitable to cause microcracks in machining of the brittle materials for their high hardness and low fracture toughness nature. The traditional damage models were constructed based on the material properties, and it was generally thought to be only dependent on grinding parameters. Based on the strain rate-sensitive analysis of brittle materials, this paper proposed new damage analysis models which consider the effect of both strain rate and grinding parameters on grinding damages. By

introducing the strain rate brought by the grinding speed and chip thickness, the new damage models were further updated as a function of the grinding speed and chip thickness. Thus, the new grinding damage models considering both the effect of strain rate and interaction depth were established. Experiments on the SEM observations and surface roughness results are used to verify the proposed model. Moreover, the new critical chip thickness model of damage-free grinding are discussed to provide further application of high-quality grinding.

The following conclusion can be drawn from this paper:

1. The increase of the grinding wheel speed can diminish the grinding damage for SiC while not deteriorating subsurface damage. Moreover, the surface roughness keeps a stable improvement with the increase of wheel speed and more plastic deformation not fracture cracks in the ground surface can be observed under a higher grinding speed.
2. The reduction of the chip thickness will help to improve the surface quality and achieve damage-free surface by reducing the surface damages. Moreover, the subsurface damage is lesser when the chip thickness decreases.
3. In the study of damage-free grinding of brittle materials, the critical depth for ductile grinding of SiC can be greatly improved through a combination of the increase of the wheel speed and the control of chip thickness. This will also help to substantially increase the material removal rate while not sacrificing the machining quality.

**Funding** This work is supported by the National Major Projects (2013ZX04001-141), National High Technology Research and Development Program of China (2012AA041309), Innovation Funds of Donghua University (CUSF-DH-D-2015100) and Morris M. Bryan Jr. Professorship for Advanced Manufacturing Systems in Georgia Institute of Technology. The authors wish to record their gratitude to their generous supports.

## References

1. Agarwal S, Rao PV (2011) Improvement in productivity in SiC grinding *ProcIMechE Part B. J Eng Manuf* 225(B6):811–830
2. Chongjun W, Beizhi L, Jingzhu P, Liang SY (2016) Ductile grinding of silicon carbide in high speed grinding. *Journal of Advanced Mechanical Design, Systems, and Manufacturing* 10:2
3. Chongjun Wu, Beizhi Li, Jianguo Yang and Steven Y Liang (2016). Prediction of grinding force for brittle materials considering co-existing of ductility and brittleness. *Int J Adv Manufact Tech.* 1–9. doi: 10.1007/s00170-016-8594-4.
4. Brinksmeier E, Mutlugünes Y, Klocke F, Aurich JC, Shore P, Ohmori H (2010) Ultra-precision grinding. *CIRP Ann Manuf Technol* 59(2):652–671
5. Yue C, Liu X, Ma J, Liu Z, Liu F, Yang Y (2014) Hardening effect on machined surface for precise hard cutting process with consideration of tool wear. *Chinese J Mech Eng* 27(6):1249–1256



6. Li B, Ni J, Yang J, Liang SY (2014) Study on high-speed grinding mechanisms for quality and process efficiency. *Int J Adv Manuf Technol* 70(5–8):813–819
7. Malkin S, Hwang TW (1996) Grinding mechanisms for ceramics. *CIRP Ann Manuf Technol* 45(2):569–580
8. Li HN, Yu TB, Zhu LD, Wang WS (2016) Evaluation of grinding-induced subsurface damage in optical glass BK7. *J Mater Process Technol* 229:785–794
9. Lawn BR, Evans AG, Marshall DB (1980) Elastic/plastic indentation damage in ceramics: the median/radial crack system. *J Am Ceram Soc* 63:574–581
10. Lambropoulos JC, Fang T, Funkenbusch PD, Jacobs SD, Cumbo MJ, Golini D (1996) Surface micro roughness of optical glasses under deterministic microgrinding. *Appl Opt* 35(22):4448–4462
11. Li SY, Wang Z, Wu YL (2008) Relationship between subsurface damage and surface roughness of optical materials in grinding and lapping processes. *J Mater Process Technol* 205:34–41
12. Yao ZQ, Gua WB, Li KM (2012) Relationship between surface roughness and subsurface crack depth during grinding of optical glass BK7. *J Mater Process Technol* 212:969–976
13. Gu W, Yao Z, Li K (2011) Evaluation of subsurface crack depth during scratch test for optical glass BK7. *Proc IMechE, Part C: J Mech Eng Sci* 225(12):2767–2774
14. Lin XH, Ke XL, Ye H, Hu CL, Guo YB (2016) Investigation of surface/subsurface integrity and grinding force in grinding of BK7 glass *Proc IMechE Part C: J Mech Eng Sci* 0954406216631575
15. Ramesh K, Huang H (2006) Use of wheel speed as a parameter to inhibit surface crack generation in the grinding of wear-resistant fillers. *Int J Adv Manuf Technol* 28:701–706
16. Wang CC, Fang QH, Chen JB, Liu YW, Jin T (2016) Subsurface damage in high-speed grinding of brittle materials considering kinematic characteristics of the grinding process. *Int J Adv Manuf Technol*. doi:10.1007/s00170-015-7627-8
17. Ravichandran G, Subhash G (1995) A micromechanical model for high strain rate behavior of ceramics. *Int J Solids Struct* 32(17, 18):2627–2646
18. Hall IW, Guden M (1998) High strain rate behavior of a SiC particulate reinforced Al<sub>2</sub>O<sub>3</sub> ceramic matrix composite. *Scr Mater* 38(4):667–674
19. Jing X, Maiti S, Subhash G (2007) A new analytical model for estimation of scratch-induced damage in brittle solids. *J Am Ceram Soc* 90(3):885–892
20. Zhu D, Yan S, Li B (2014) Single-grit modeling and simulation of crack initiation and propagation in SiC grinding using maximum undeformed chip thickness. *Comput Mater Sci* 92:13–21
21. Chongjun W, Beizhi L, Jianguo Y, Liang SY (2016) Experimental investigations of machining characteristics of SiC in high speed plunge grinding. *J Ceram Process Res* 17(3):223–231
22. Malkin S (1989) *Grinding technology, theory and applications of machining with abrasives*. Ellis Horwood Limited, Chichester
23. Lin S, Yang S, Lin Y, Zhao P, Wu P, Jiang Z (2015) A new model of grinding forces prediction for machining brittle and hard materials. *Procedia CIRP* 27:192–197
24. Liu Y, Li B, Wu C, Zheng Y (2015) Simulation-based evaluation of surface micro-cracks and fracture toughness in high-speed grinding of silicon carbide ceramics. *Int J Adv Manuf Technol*. doi:10.1007/s00170-015-8218-4
25. Pan Z, Liang SY, Garmestani H, Shih DS (2016) Prediction of machining-induced phase transformation and grain growth of Ti-6Al-4 V alloy. *Int J Adv Manuf Technol*. doi:10.1007/s00170-016-8497-4
26. Lankford J (1981) Mechanisms responsible for strain-rate-dependent compressive strength in ceramic materials. *J Am Ceram Soc* 64(2):C-33–C-34
27. Bifano TG, Dow TA, Scattergood RO (1991) Ductile-regime grinding: a new technology for machining brittle materials. *J Eng Ind Trans ASME* 113(2):184–189
28. Ding Z, Li B, Liang SY (2015) Maraging steel phase transformation in high strain rate grinding. *Int J Adv Manuf Technol* 80:711–718